Modeling of Ionic Transfer Across a Diaphragm In a Batch Acidified Copper Sulphate Electrochemical Reactor

Amer D. Zmat
College of Engineering, University of Al-Qadisiyah

Abstract

A mixed copper sulphate/ H_2SO_4 electrolyte was operated in a galvanostatic mode, where hydrogen ions produced at the anode compartment due to water dissociation on anode then transferred with copper ions across the diaphragm of electrochemical reactor into cathode compartment. Series of runs were made using an electrolyte of concentration 0.2M $CuSO_4$/1.0M H_2SO_4 and 0.4M $CuSO_4$/1.0M H_2SO_4. The cell was operated at different current densities (0.03, 0.06 and 0.12A/cm^2).Both anolyte and catholyte copper and acid concentrations were measured by atomic absorption technique. The concentration of copper ions Cu^{+2} in the catholyte was found to be decreased with time due to copper deposition and its concentration in the anolyte also decreased due to the transfer of Cu^{+2} across the diaphragm from the anode compartment to the cathode compartment but with a less gradient. As the electrolysis proceeds, the hydrogen evolution increases and the copper deposition efficiency decreases. Predicted copper deposition at constant current density and higher initial copper ion concentration gave satisfactory agreement with experimental data.

KEYWORDS: electrochemical reactor, electrochemical modeling, diaphragm, Ionic solution, electro migration.

الخلاصة

يهدف البحث الى تمثيل الانتقال الايوني من خلال الاغشية في المفاعلات الالكتركيمياوية نوع مفاعلات الوجبة لمحلول كبريتات النحاس بوجود حامض الكبريتيك. تم اجراء التفاعل بطور galvanostatic ، حيث يتحرر الهيدروجين في جناح الانود نتيجة تفكك الماء وتنتقل ايونات الهيدروجين من جناح الانود الى جناح الكاثود في حين وجد ان تركيز ايونات النحاس تقل كدالة للزمن نتيجة ترسيبها على الكاثود وكذلك تقل ايونات النحاس في الانود نتيجة الانتقال بالانتشار وفرق التركيز. تم اجراء مجموعتين من التجارب المختبرية الاولى بتركيز (0.2M $CuSO_4$/1.0M H_2SO_4) والثاني (0.4M $CuSO_4$/1.0M H_2SO_4) وتحت شدة تيار مختلفة (0.03, 0.06 and 0.12A/cm^2). تم استخدام جهاز الامتصاص الذري لقياس التراكيز وبينت النتائج المتحققة تقارب ملموس بين النتائج العملية والنتائج التي حققها الموديل.

Introduction

Ionic transfer takes place across a diaphragm due to the concentration difference between the two compartments and the migration due to potential gradient. In many cases where the cathodic process is the important reaction, evolution of O_2 is the main anodic reaction. The anodic reaction causes an increase in hydrogen ions concentration in the anolyte. The transfer of hydrogen ions to the catholyte will occur due to migration and diffusion. The consequent increase in hydrogen ion concentration in the catholyte can cause a decrease in the current efficiency for the main cathodic process due to co-evolution of H_2[David J.Pickett, 1977]. [Wilke et al, 1953] had measured the limiting currents on plane, vertical cathodes from unstirred solutions. They have estimated the concentration of the sulphuric acid at the electrode to the rate of transport of the acid away from the electrode by diffusion and convection. [Holems and R. Wilke, 1963] had studied the convective mass transfer in a diaphragm diffusion cell, both free and forced convection. The mass transfer characteristics of a vertical diaphragm cell were investigated and the results were correlated in term of stirred speed and fluid properties, they concluded that operation above a critical stirred speed is appropriate for a number of common systems but that significance errors can arise for system of high viscosity and low diffusivity. [Newman , 1966] had studied the effect of ionic migration on limiting currents for several electrolytic solutions. For the case of $CuSO_4$ and H_2SO_4, the effect of migration was treated with assumption that bisulphate ions were completely dissociated .[Selman and Newman, 1971] have dealt with the mass transfer to vertical surface in free convection and the effect of ionic migration on limiting current. The diffusion layer thickness is greater for H_2SO_4 than for the $CuSO_4$ on account of the larger

value of the diffusion coefficient of H^+ ions. Thus the density difference in the outer part of the diffusion layer is positive while it is negative near the electrode.[IbI and Dossenbach, 1983] had studied the convective mass transfer in electrolysis of $CuSO_4/H_2SO_4$ system in a cell with two plane, parallel, copper electrodes with laminar flow parallel to both electrodes. The concentration of sulphuric acid was much larger than that of the copper sulphate so that the migration of Cu^{+2} ions was negligible. [Tozawa et al, 1983] had studied the effect of the second dissociation of sulphuric acid on electrical conductivities of the mixed electrolytes.

[IR. J. H. G. Van Der Stegen, 1989] investigated the Models and equations that describing aspects of diaphragm performance for the chlorine-caustic system. They found that excellent control of wettability and, therefore, of the amount of gases inside the diaphragm, together with chemical resistance to the environment during electrolysis are an essential prerequisite to performances of non-asbestos diaphragms that are comparable to those of asbestos diaphragms. [Roberto Vidal et al., 1994] described a model of the homogeneous chemistry and transport processes within the separator of a chrome-alum electro winning cell, they found that convection was the dominant mode of transport for the experimental conditions and the Simulation results explain experimental observations concerning an apparent disappearance of dichromate ions produced at the cell anode. [W. Richard Bowen and Julian S. Welfoot, 2002] described a model allowing calculation of uncharged solute rejection on the basis of a single membrane parameter (pore radius). The theoretical description is based on a hydrodynamic model of hindered solute transport in pores. They concluded that the good agreement between their model with experimental data confirms that uncharged solute rejection in nanofiltration membranes may be well-described by such a continuum model. [V. Nikonenko, et.al, 2002] studied the mathematical model of ion transport in membrane systems, Different scales of ion transport were considered: 1) in the membrane, where two approaches are used, the irreversible thermodynamics and modeling of the membrane material, the last permits to link physicochemical properties with structure-kinetic parameters of the membrane; 2) in a three-layer system composed of a membrane with two adjoining diffusion layers; and 3) in an electro dialysis 2D cell, where the differential equation of convective diffusion is used. [Jesus Garcia-Aleman and James Dickson, 2004]made a side-by-side comparison of the performance of McMaster pore-filled (MacPF) and commercial nanofiltration (NF) membranes, a pseudo two-dimensional model based on the extended Nernst–Planck equation, a modified Poisson–Boltzmann equation, and hydrodynamic calculations was adopted .Their results demonstrated that the rejection and transport mechanisms are the same in the commercial and MacPF membranes with different contributions from each type of mechanism (convection, diffusion and electro migration). [Paula Moon et al. , 2004] described the transport of ions and dissociation of a single salt and a solvent solution in an electro dialysis (ED) stack. The ED stack basic unit was made of a two-compartment cell: dilute and concentrate, they proposed and analyzed three model formulations for a single salt (KCl). The first and the second models were for a one- and two-dimensional continuous ED, and the third examined batch ED. They examined the diffusion and electro migration of ions in the polarization region and consider electro migration and convection in the bulk region. They showed that the ionic surface concentration of both membranes in the dilute compartment is affected by two parameters: flow rate and current density.

Later on [Kanchan Mondal et al. , 2010] had developed a mathematical model for the removal of impurities of the metal ions of Fe, Ni, and Cu from hard chromium plating solution by electro migration through the diaphragm and subsequent electro deposition .They found that the experimental data were closely match results predicted from the model

developed. The inherent model parameters such as mobility, diffusivity, mass transfer coefficient and metal deposition rate constants were estimated.

The aim of the present work is to develop a mathematical model for the ionic transfer across a diaphragm in a batch acidified copper sulphate electrochemical reactor. Both copper and hydrogen concentration profiles will be studies and compared to experimental data.

Experimental Work

The cell used for acidified $CuSO_4/H_2SO_4$ system is shown in figure (1). It was constructed from glass sheets of 6 mm thickness. The internal dimensions of the cell are 7.5 cm length, 6.3 cm width and 5.8 cm depth. The cell was divided into tow compartments. The first is cathode chamber (78.5 cm^3) and the second is anode chamber (109 cm^3). Both electrodes and diaphragm have equal areas (30cm^2). The electrodes were made of (lead-6%Antemony alloy) and copper sheets working as anode and cathode respectively. Both sheets are rectangular and of 3 mm thickness. The diaphragm material used in this work was polyester A (filter cloth of 75 μ thickness and equivalent pore radius 9.1 μ). A power supply (10A, 30V) was used. The positive terminal of the power supply was connected to the anode and the negative terminal was connected to the cathode. The experiments were undertaken using 0.2M $CuSO_4$/1.0M H_2SO_4 and 0.4M $CuSO_4$/1.0M H_2SO_4 as electrolyte. Acid and copper concentrations were measured for each run at different periods of time. 1 ml samples were withdrawn from the ends and the center of the cell using 1 ml pipette at regular time intervals. The cell was operated at different constant current densities (0.03A/cm^2, 0.06A/cm^2, and 0.12A/cm^2); the electrolyte solutions were prepared from analytical grade cupric sulphate and sulphuric acid. The $CuSO_4$ samples were analyzed by atomic absorption technique.

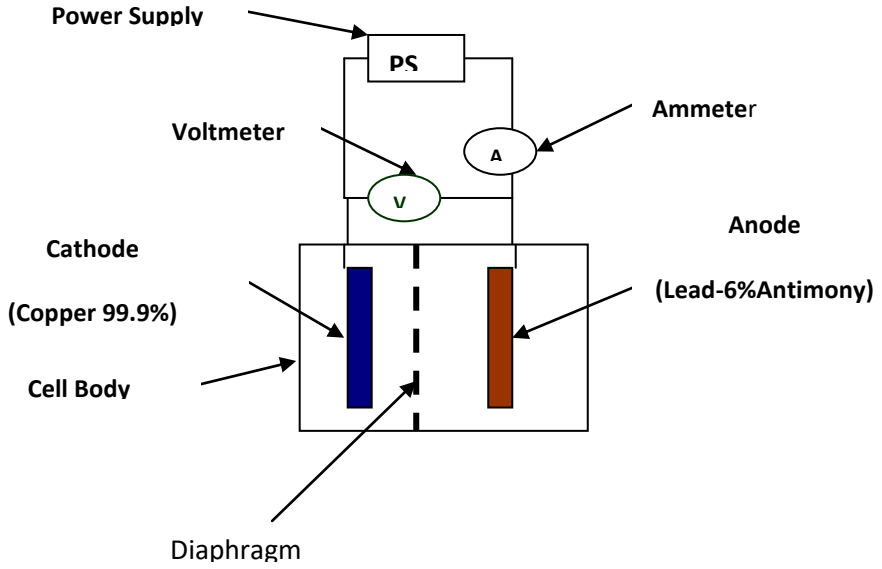

Figure (1) the schematic diagram of $CuSO_4/H_2SO_4$ system.

Mathematical Modeling:

For the $CuSO_4/H_2SO_4$ system, the reaction that takes place at the anode surface is the oxidation of water (oxygen evolution).

$$H_2O - 2e \longrightarrow 1/2\ O_2 + 2H^+ \qquad (1)$$

The production of hydrogen ions at the anode will cause a gradual rise in H^+ concentration in the catholyte due to the migration and diffusion fluxes across the diaphragm. Since the total rate of consumption of H^+ at the cathode is lower than the rate of H^+ production at the anode. Diffusion of hydrogen species across the diaphragm from the anolyte to the catholyte will

occur. As the electrolysis proceeds, the Cu^{+2} ions will decrease in the catholyte due to the copper deposition at the cathode. Cu^{+2} diffusion from the anolyte to the catholyte across the diaphragm will take place and cause a decrease in Cu^{+2} concentrations in the anolyte. A model of two-compartment reactor was developed. Material balances were set up for the anode and cathode compartments separately, and then they were linked in terms of the ionic transfer across the diaphragm. The ions under consideration in this system are H^+, HSO_4^-, SO_4^{-2} and Cu^{+2}. They are represented by the subscripts 1, 2, 3 and 4 respectively. C and Cu refer to the stoichimetric concentration of H_2SO_4 and $CuSO_4$ respectively [1]. Figures (2&3) show the schematic diagram of a batch electrochemical reactor and schematic representation of fluxes of the ions through the diaphragm respectively. N_1 (H^+), N_2 (HSO_4^-), N_3 (SO_4^{-2}) and N_4 (Cu^{+2}) indicate those fluxes of ions.

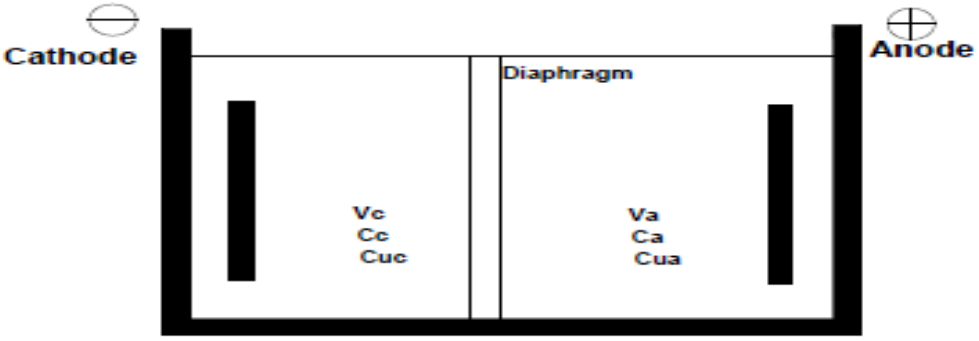

Figure (2) batch electrochemical reactor

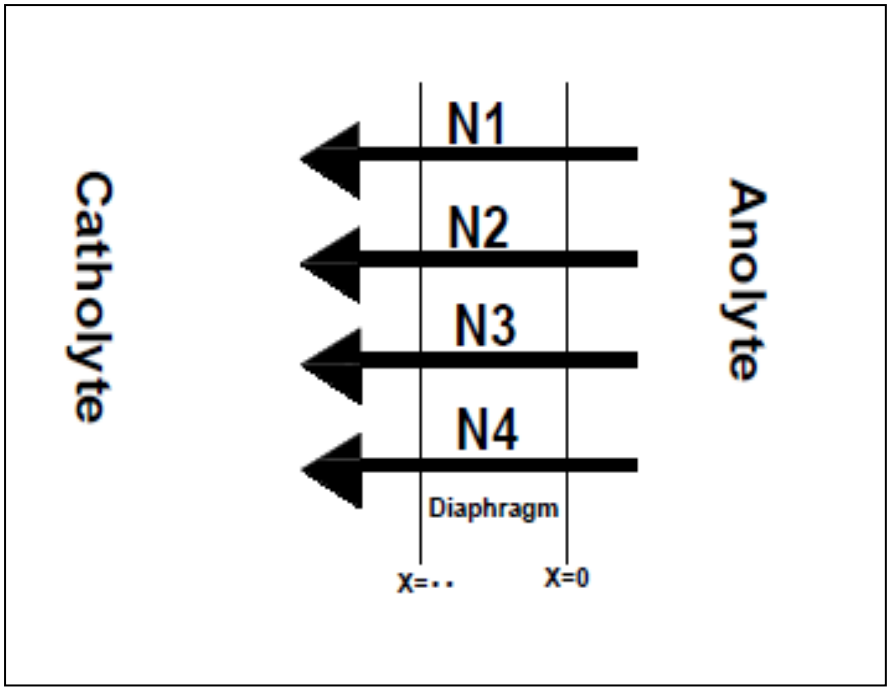

Figure (3) Fluxes across the diaphragm in $CuSO_4/H_2SO_4$ system.

The combined fluxes N_1+N_2 and N_2+N_3 are constants across the diaphragm. Also the Cu^{+2} ions are conserved during the passage through the diaphragm, therefore N_4 is constant. The

rate of transfer of charge per unit area through the solution can be represented by the following equation:

$$i = F\Sigma N_j.Z_j \quad (2)$$

Where:

$N_{j\ is}$ the flux of species j (mol/m^2.s)

Z_j is the charge number of species j

F is the Faraday's constant.

Rewriting equation (2) for the $CuSO_4/H_2SO_4$:

$$\frac{i}{F} = (N_1 + N_2) - 2(N_2 + N_3) + 2N_4 \quad (3)$$

$$N_1 = D_1 \frac{dC_1}{dx} - D_1C_1E + C_1.V \quad (4)$$

$$N_2 = -D_2 \frac{dC_2}{dx} + D_2C_2E + C_2.V \quad (5)$$

$$N_3 = -D_3 \frac{dC_3}{dx} + 2D_3C_3E + C_3.V \quad (6)$$

$$N_4 = -D_4 \frac{dC_4}{dx} - 2D_4C_4E + C_4.V \quad (7)$$

Where:

D_i is the diffusion coefficient of species (i).

C_i is the concentration of species (i).

E is the potential gradient parameter

V is the fluid velocity across the diaphragm.

The concentration of H^+, HSO_4^-, SO_4^{-2} and Cu^{+2} ions can be written in terms of H_2SO_4 and $CuSO_4$ concentrations (C, Cu):

C_1=KC (8)

C_2=(2-k)C (9)

C_3=(k-1)C + Cu (10)

C_4= Cu (11)

Where:

K is the proportionality constant of H_2SO_4 dissociation $(\frac{C_{H^+}}{C_{H_2SO_4}})$.

Accordingly, the combined fluxes equations become:

$$N_1 + N_2 = -k_1 \frac{dC}{dx} - k_2CE + 2CV \quad (12)$$

$$N_2 + N_3 = -k_3 \frac{dC}{dx} - D_3 \frac{dCu}{dx} + k_4CE + 2D_3Cu.E + Cu.V + C.V \quad (13)$$

$$N_4 = -D_4 \frac{dCu}{dx} - 2D_4Cu.E + Cu.V \quad (14)$$

Substituting for (N_2+N_3) in equation (13) from equation (3):

$$N_1 + N_2 + 2N_4 - \frac{i}{F} = -2k_3 \frac{dC}{dx} + 2k_4C.E + 2C.V - 2D_3 \frac{dCu}{dx} + 2D_3Cu.E + 2Cu.V \quad (15)$$

Equation (15) shows that the important model parameters are (N_1+N_2), N_4 and I. The potential gradient parameter E can be eliminated from equation (15) using the following equation:

$$E = -\frac{1}{2Cu}\frac{dCu}{dx} - \frac{N_4}{2D_4Cu} + \frac{V}{2D_4} \quad (16)$$

Substituting into equation (15) and rearrange:

$$\frac{dC}{dx} = k_5 - k_6\frac{C}{Cu} - (k_7 + k_8\frac{C}{Cu})\frac{dCu}{dx} + k_9C.V + k_{10}Cu.V \quad (17)$$

Where:

$$k_5 = \frac{i}{2Fk_3} - \frac{(N_1+N_2)}{2k_3} - \frac{N_4}{k_3}(1+\frac{D_3}{D_4}) \quad (18)$$

$$k_6 = \frac{N_4k_4}{2k_3D_4} \quad (19)$$

$$k_7 = \frac{2D_3}{k_3} \quad (20)$$

$$k_8 = \frac{k_4}{2k_3} \quad (21)$$

$$k_9 = \frac{(1+\frac{k_4}{2D_4})}{k_3} \quad (22)$$

$$k_{10} = \frac{(1+\frac{D_3}{D_4})}{k_3} \quad (23)$$

For $\frac{dCu}{dx}$:

$$\frac{dCu}{dx} = \frac{k_{11}Cu - k_{12}C + k_{13}C.Cu.V + k_{14}Cu^2.V}{k_7Cu + k_{15}C} \quad (24)$$

Where: $k_{11} = \frac{N_1+N_2}{k_1}$ (25)

$$k_{12} = k_5 + k_{11} \quad (26)$$

$$k_{13} = k_6 + \frac{k_2N_4}{2k_1D_4} \quad (27)$$

$$k_{14} = k_9 + (\frac{k_2}{2D_4} - 2)/k_1 \quad (28)$$

$$k_{15} = k_8 + \frac{k_2}{2k_1} \quad (29)$$

For the case when there is no flow a set of simple equations can be obtained by assuming the volume (v) equals (0). Then, the ionic transfer across the diaphragm will be due to migration and diffusion only.

$$\frac{dCu}{dx} = \frac{k_{11}.Cu - k_{12}.C}{k_7.Cu + k_{15}.C} \quad (30)$$

$$\frac{dC}{dx}=\frac{k_2}{2k_1}\left(\frac{k_{12}.Cu-k_{13}.C^2}{k_7.Cu^2+k_{15}.C.Cu}\right)+k_{14}.\frac{C}{Cu}-k_{11} \quad (31)$$

For batch reactor shown in figure (4), a material balance for the Cu^{+2} ions over the anode compartment gives:

$$V_A\frac{dCu_A}{dt}=-N_4A \quad (32)$$

Also, a material balance for the Cu^{+2} ions over the cathode compartment gives:

$$V_C\frac{dCu_c}{dt}=N_4A-\frac{I.\varepsilon}{2F} \quad (33)$$

Where ε represents the instantaneous current efficiency for the copper deposition. The material balance for the hydrogen ionic species over the anode compartment is set up where species are formed with 100% current efficiency.

$$2V_A\frac{dC_A}{dt}=\frac{I}{F}-(N_1+N_2)A \quad (34)$$

The corresponding material balance over the cathode compartment gives:

$$2V_C\frac{dC_c}{dt}=(N_1+N_2)A-\frac{I(1-\varepsilon)}{F} \quad (35)$$

And the total material balance gives:

$$Cu_A + Cu_C + C_A + C_C = \text{constant} \quad (36)$$

For the batch process, the fluid velocity is equal to zero, therefore no convective flux exists and the total flux across the diaphragm will be due to migration and diffusion. The migration flux of hydrogen species (N_1+N_2) can be expressed as:

$$(N_1+N_2)_m=\frac{It_1}{AF} \quad (37)$$

$$(N_1+N_2)_d=-D_1\frac{dC}{dx}=-D_1\frac{(C_C-C_A)}{\delta} \quad (38)$$

$$(N_1+N_2)_{total}=\frac{It_1}{AF}-D_1\frac{(C_C-C_A)}{\delta} \quad (39)$$

The total copper ions flux across the diaphragm is:

$$N_4=\frac{It_{Cu^{+2}}}{2AF}-D_4\frac{(Cu_c-Cu_A)}{\delta} \quad (40)$$

Using Runge-Kutta method to calculate the variations of the anolyte and catholyte concentrations for both H_2SO_4 and $CuSo_4$ with respect to time.

Results And Discussion:

Tables (1, 2, 3 and 4) summarize the experimental data obtained under galvanostatic operation. The data presented in the these tables show measured anolyte and catholyte concentrations of copper and hydrogen ions with time, the amount of deposited copper and the calculated current efficiency for each run.

It can be seen that in each run the concentration of copper ion decreases with time at the catholyte and anolyte compartments. The concentration of hydrogen ions decreased in the catholyte and increased in the anolyte, also the gradient concentration of copper ions increased with increasing current density. These behaviors may be interrupted as follows:

For the galvanostatic operation at current density ($0.03A/cm^2$), the main reaction in cathode compartments is the reduction of copper ions at the surface of the cathode, at the same time the reduction of hydrogen ions to produce the hydrogen gas occurred. The rate of copper deposition is higher than hydrogen evolution at this current density .also the rate of copper deposition is higher than the rate of copper migration from the anolyte to catholye via the

diaphragm leading to decreasing the copper ions concentration in the catholyte as the electrolysis proceeds. The gradient concentration of copper ions in catholyte is much greater than in the anolyte.

Table (1) Concentrations profiles for Cu^{+2} and H^{+} at current density ($0.03\ A/cm^2$) and initial electrolyte concentration ($0.2MCuSO_4/0.1M\ H_2SO_4$)

Time(Min.)	catholyte		Anolyte	
	Cu^{+2} conc.(M)	H^{+} conc.(M)	Cu^{+2} conc.(M)	H^{+} conc.(M)
0	0.2	2.0	0.2	2.0
10	0.172	1.996	0.191	2.1
20	0.13	1.993	0.186	2.17
30	0.121	1.985	0.18	2.25
40	0.093	1.983	0.174	2.31
50	0.085	1.98	0.168	2.35
60	0.072	1.975	0.157	2.42
Amount of Cu deposited(gm)	0.906			
Current Efficiency (%)	75 (based on electrolysis time 60 Min.)			

Table (2) Concentrations profiles for Cu^{+2} and H^{+} at current density ($0.06A/cm^2$) and initial electrolyte concentration ($0.2MCuSO_4/0.1M\ H_2SO_4$)

Time(Min.)	catholyte		Anolyte	
	Cu^{+2} conc.(M)	H^{+} conc.(M)	Cu^{+2} conc.(M)	H^{+} conc.(M)
0	0.2	2.0	0.2	2.0
10	0.166	1.99	0.183	2.08
20	0.121	1.98	0.17	2.16
30	0.105	1.97	0.162	2.26
40	0.078	1.96	0.155	2.41
50	0.055	1.94	0.145	2.5
60	0.042	1.94	0.137	2.61
Amount of Cu deposited(gm)	1.375			
Current Efficiency (%)	63 (based on electrolysis time 60 Min.)			

Table (3) Concentrations profiles for Cu^{+2} and H^{+} at current density ($0.12\ A/cm^2$) and initial electrolyte concentration ($0.2MCuSO_4/0.1M\ H_2SO_4$)

Time(Min.)	catholyte		Anolyte	
	Cu^{+2} conc.(M)	H^{+} conc.(M)	Cu^{+2} conc.(M)	H^{+} conc.(M)
0	0.2	2.0	0.2	2.0
10	0.16	1.99	0.177	2.15
20	0.11	1.97	0.152	2.2
30	0.082	1.95	0.141	2.3
40	0.053	1.91	0.123	2.4
50	0.044	1.94	0.115	2.53
60	0.033	2.1	0.1	2.65
Amount of Cu deposited(gm)	1.964			

Current Efficiency (%)	45 (based on electrolysis time 60 Min.)

Table (4) Concentrations profiles for Cu^{+2} and H^{+} at current density (0.03 A/cm^2) and initial electrolyte concentration (04M$CuSO_4$/0.1M H_2SO_4)

Time(Min.)	catholyte		Anolyte	
	Cu^{+2} conc.(M)	H^{+} conc.(M)	Cu^{+2} conc.(M)	H^{+} conc.(M)
0	0.4	2.0	0.4	2.0
10	0.371	1.99	0.395	2.1
20	0.32	1.988	0.392	2.15
30	0.29	1.982	0.390	2.21
40	0.28	1.98	0.385	2.35
50	0.26	1.978	0.382	2.4
60	0.232	1.976	0.378	2.43
Amount of Cu deposited(gm)		1.0518		
Current Efficiency (%)		88 (based on electrolysis time 60 Min.)		

At the anode the dissociation of water take place with increasing rate leading to production of hydrogen ions. The rate of hydrogen ions formation was greater than the hydrogen migration through the diaphragm so that the concentration of hydrogen increases as the electrolysis proceeds in the anolyte while decreases slowly in the catholyte because of the difference between the rate of migration and rate of reduction at the cathode. When the time of electrolysis exceeded 60 min the concentration of hydrogen ions may be raised and exceeded the initial values in the catholyte but the current efficiency dropped much higher making the process not economic from industrial point of view. Figure (3) shows the concentration profile of copper ions during the galvanostatic operation at (0.03A/cm^2).

For the galvanostatic operations at current densities higher than (0.03A/cm^2).the rate of hydrogen evolution at the cathode will be proceeded at higher rates leading to lowering the current efficiency, however, the general behavior of concentration profiles were the same. Figures (4, 5) show the profiles at 0.06and 0.12A/cm^2 respectively.

The copper deposits obtained at current density (0.03A/cm^2)was compact and coherent while a fragile deposit obtained at current density (0.06A/cm^2)the reason may be the effect of hydrogen bubbles produced at the cathode surface which penetrated the deposits .at current density (0.12A/cm^2) a spongy and powdery deposits was obtained .

The concentration profiles at current density (0.03A/cm^2) and initial electrolyte concentration (0.2M $CuSO_4$/1.0M H_2SO_4) were considered for comparison between the experimental and model results

Figure(6) shows the concentration profiles for copper ion concentrations at the catholyte and anolyte .The results indicate that a well match between the experimental and theoretical values .This may be contributed to the high current efficiency (75%)obtained which means a less contribution for hydrogen evolution on the convective and diffusion rates across the diaphragm. therefore operating at lower current density or higher initial concentration of copper ions leads to a good agreements between the experimental data and model and this clearly observed at initial concentration of electrolyte(0.4M $CuSO_4$/1.0M H_2SO_4) as shown in figure(7)where higher current efficiency (88%) was obtained.

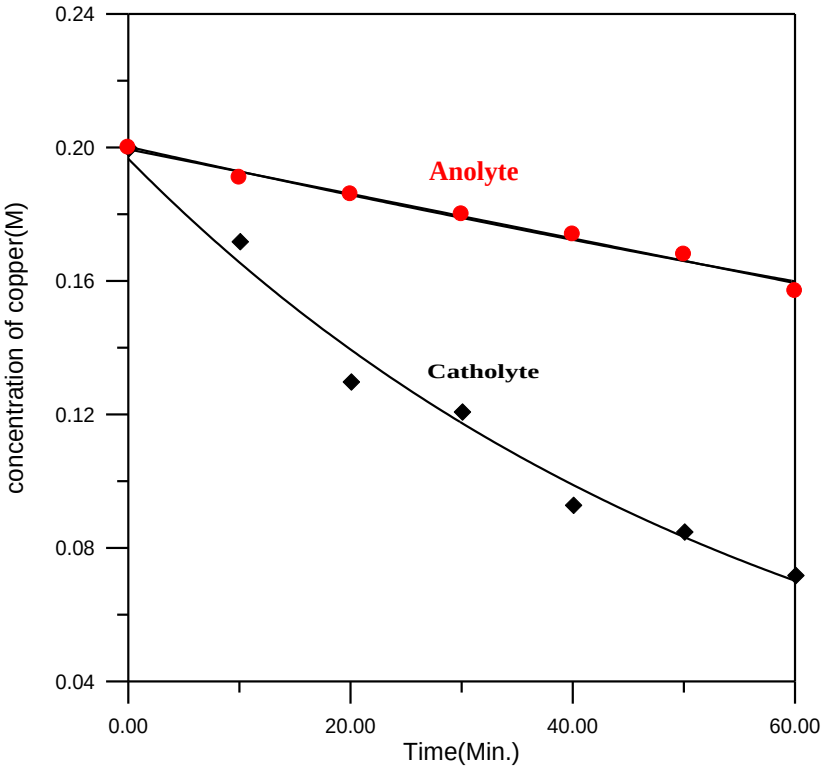

Fig.(3) concentration profiles at current density(0.03A/cm^2) and intail electrolyte concentration(0.2MCuSO4/1.0M H2SO4)

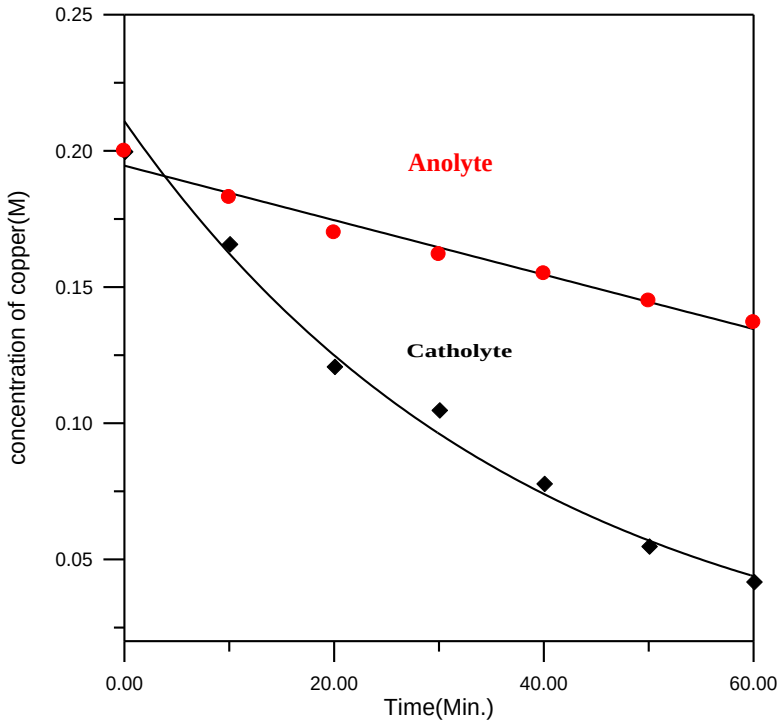

Fig.(4) concentration profiles at current density(0.06A/cm^2) and intail electrolyte concentration(0.2MCuSO4/1.0M H2SO4)

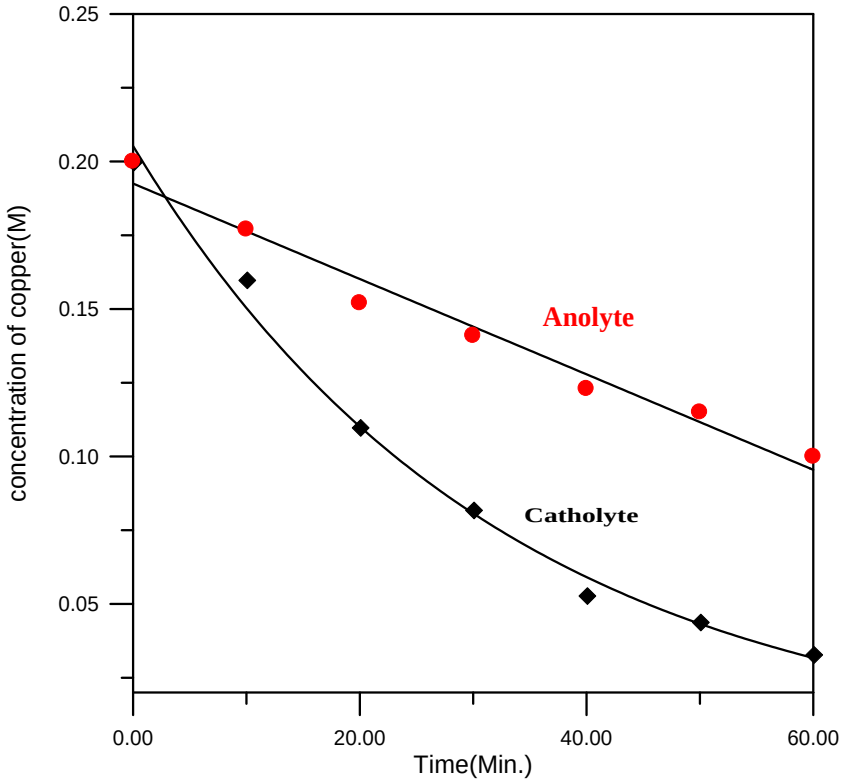

Fig.(5)concentration profiles at current density(0.12A/cm^2) and intail electrolyte concentration(0.2MCuSO4/1.0M H2SO4)

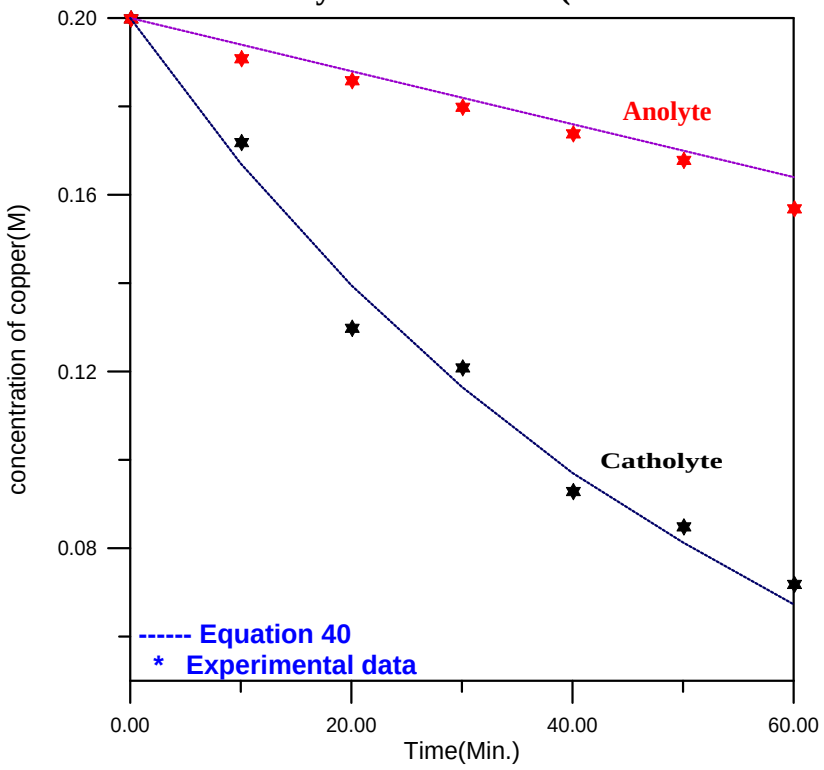

Fig.(6) concentration profiles at current density(0.03A/cm^2) and intail electrolyte concentration(0.2MCuSO4/1.0M H2SO4)

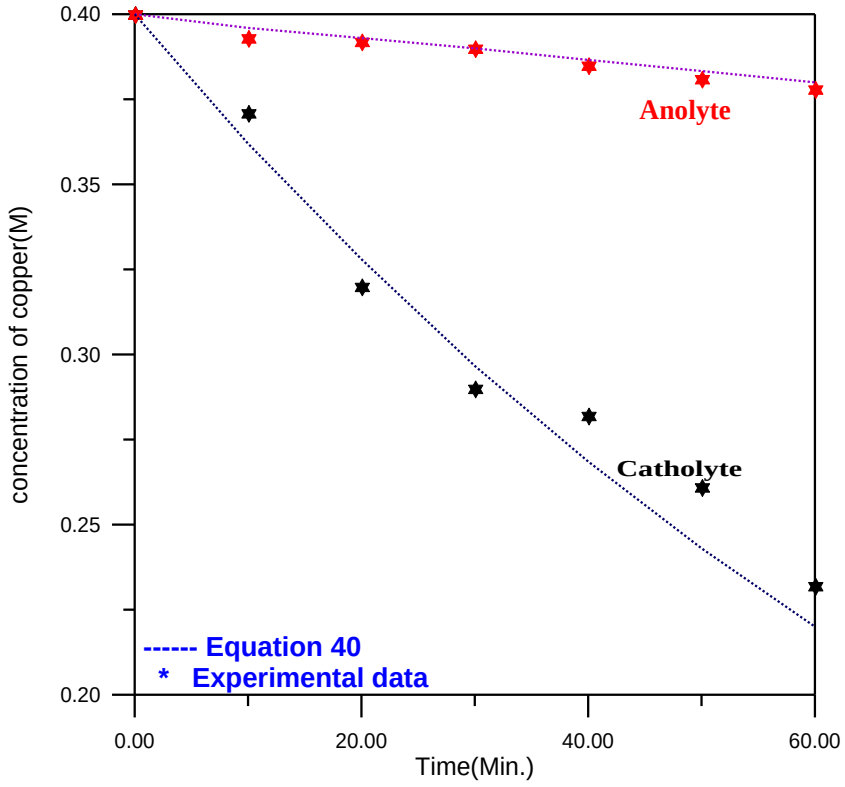

Fig.(7) concentration profiles at current density(0.03A/cm^2) and intail electrolyte concentration(0.4MCuSO4/1.0M H2SO4)

Conclusion

The galvanostatic operation can be adopted for the batch electrochemical reactor operated at lower current density and higher metal ion concentration where a higher current efficiency could be obtained. The galvanostatic operation nearby the limiting current density gives satisfactory agreement between the predicted and experimental data. The concentration gradient of copper ions is higher in the catholyte than anolyte due to electro deposition. The operations at higher concentrations led to a slightly change in concentration of metal ion at the anolyte not exceeded 5% and it could be considered constant during the operation. The effect of migration due to potential difference is more pronounced on the ionic mass transfer across the diaphragm than convective in batch reactor.

References

David J.Pickett, 1977, "Electrochemical Reactor Design "Elsevier, New York.

Wilke,C.R.,Eisenberg ,M and Tobias ,C.W., 1953, "Limiting current technique for unstirred solution" ,J. Electrochemical society,100(11),513.

John,Holems,Charls R.Wilke and Donald R. Olendar, 1963, "Convective Mass Transfer In A diaphragm Diffusion Cell",*J. Phys. Chem.*, *67* (7), pp 1469–1472.

Newman, J., 1966, ' Ind.Eng.Chem'. 5,525.

Selman, J.R. and Newman, J., 1971, ' J. Electrochemical society', 118, 1070.

IbI, N.and Dossenbach, O., 1983, "convective mass transport" Yeager, New York .

Tozawa,K,Sasaki,K.and Umestu,Y., 1983, Hydrometall.Res,Dev,Plant Pract.,Proc.3ed Int. Symp.

IR. J. H. G. Van Der Stegen, 1989, ”Mass transfer and structure of asbestos and non-asbestos diaphragms for chlorine and caustic production “, Journal of Applied Electrochemistry, Volume 19, Number 4 .

Roberto Vidal, Paul Duby and Alan C. West, 1994, ”A mathematical model of ionic transport in a porous diaphragm of a chrome-alum cell Metallurgical and Materials Transactions B, Volume 25, Number 3 .

W. Richard Bowen, Julian S. Welfoot, 2002, " Modeling the performance of membrane nanofiltration —critical assessment and model development", *Chemical Engineering Science, Volume 57, Issue 7*.

V. Nikonenko, V. Zabolotsky, C. Larchet, B. Auclair, G. Pourcelly, 2002, ” Mathematical description of ion transport in membrane systems “,*Desalination, Volume 147, Issues 1-3*.

Jesus Garcia-Aleman, James Dickson, A. Mika, 2004, ” Experimental analysis ,modeling and theoretical design of McMaster pore-filled nanofiltration membranes *Journal of Membrane Science, Volume 240, Issues1*..

Paula Moon, Giselle Sand, Deborah Stevens, Riza Kizilel , 2004, ” Computational Modeling of Ionic Transport in Continuous and Batch Electrodialysis”, Separation Science and Technology , *Volume 240, Issues 1-2*.

Kanchan Mondal, Jayasree Pattanayak, Tomasz S. Wiltowski, Shashi B. Lalvani, Nenad V. Mandich , 2010, ” Modeling of a process for removal of metal ions by electromigration and electro deposition “,the Canadian journal of chemical engineering, vol80,issu3,pages465-471.